

Shallow subsurface structure of the Vulcano-Lipari volcanic complex, Italy, constrained by helicopter-borne aeromagnetic surveys

Shigeo Okuma¹ Tadashi Nakatsuka¹ Masao Komazawa¹ Mitsuhiro Sugihara¹
Shun Nakano¹ Ryuta Furukawa¹ Robert Supper²

Key Words: subvolcanic structure, magnetic anomaly, aeromagnetic survey, Vulcano, Lipari, Aeolian Islands

ABSTRACT

Helicopter-borne aeromagnetic surveys at two different times separated by three years were conducted to better understand the shallow subsurface structure of the Vulcano and Lipari volcanic complex, Aeolian Islands, southern Italy, and also to monitor the volcanic activity of the area. As there was no meaningful difference between the two magnetic datasets to imply an apparent change of the volcanic activity, the datasets were merged to produce an aeromagnetic map with wider coverage than was given by a single dataset. Apparent magnetisation intensity mapping was applied to terrain-corrected magnetic anomalies, and showed local magnetisation highs in and around Fossa Cone, suggesting heterogeneity of the cone. Magnetic modelling was conducted for three of those magnetisation highs.

Each model implied the presence of concealed volcanic products overlain by pyroclastic rocks from the Fossa crater. The model for the Fossa crater area suggests a buried trachytic lava flow on the southern edge of the present crater. The magnetic model at Forgia Vecchia suggests that phreatic cones can be interpreted as resulting from a concealed eruptive centre, with thick latitic lavas that fill up Fossa Caldera. However, the distribution of lavas seems to be limited to a smaller area than was expected from drilling results. This can be explained partly by alteration of the lavas by intense hydrothermal activity, as seen at geothermal areas close to Porto Levante. The magnetic model at the north-eastern Fossa Cone implies that thick lavas accumulated as another eruption centre in the early stage of the activity of Fossa. Recent geoelectric surveys showed high-resistivity zones in the areas of the last two magnetic models.

INTRODUCTION

The Aeolian Island Arc is located in the Tyrrhenian Sea, southern Italy, and is composed of seven volcanic islands: Alicudi, Filicudi, Salina, Lipari, Vulcano, Panarea, and Stromboli from west to east (Figure 1). The volcanic activity of the islands is thought to originate from the subduction of the African Plate

beneath the European Plate at the southern edge of the Tyrrhenian Sea (Gasparini et al., 1982). Since ancient Greek times, Stromboli in particular has been noted for its effusive eruptions of mainly lava products, and Vulcano was noted for its violent "Vulcanian" eruptions that emitted large quantities of volcanic bombs and ash.

Activity at Vulcano has been unusually quiet since the last eruption took place between 1880 and 1890. This relatively long period of inactivity has caused concern that a future eruption could be explosive and cause severe damage. To predict and mitigate future eruptions, it is important to know the detailed subsurface structure of the volcano as well as to monitor its activity. Barberi et al. (1994) conducted a geophysical study in the central sector of the Aeolian Arc, collecting gravity, magnetic, and volcanological data, and focused chiefly on revealing the deep subsurface structure of the arc. Helicopter-borne aeromagnetic surveys have been conducted at two different times to help better understand the shallow subvolcanic structure of the Vulcano and Lipari complex, and to monitor the volcanic activity of the area (Supper et al., 2001, 2004; Okuma et al., 2003). The aim of this study is to interpret the aeromagnetic data in terms of the shallow structure of the Vulcano-Lipari complex.

GEOLOGICAL SETTING

The Vulcano and Lipari volcanic complex belongs to the Aeolian volcanic island arc and is located inside a regional graben structure aligned with the NNW-SSE trending Tindari-Letojanni

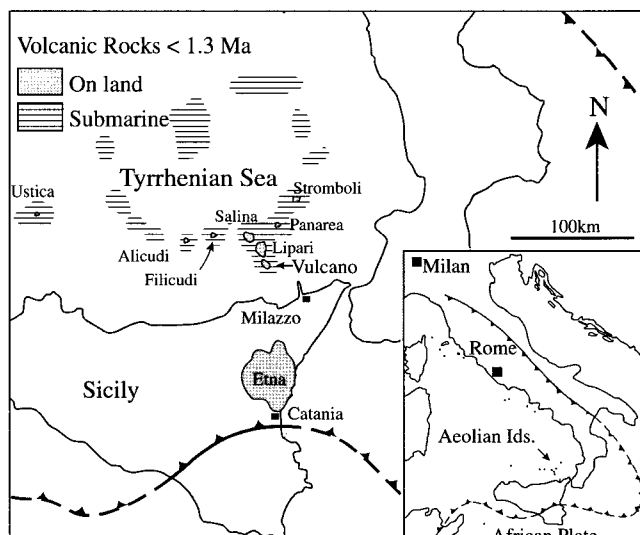


Fig. 1. The map of the study area shows the Aeolian Islands located between Sicily and the southern tip of the Italian Peninsula in the Tyrrhenian Sea. It also indicates the distribution of volcanic rocks of the age younger than 1.3 Ma (after Furukawa et al., 2000).

¹ Geological Survey of Japan, National Institute of Advanced Industrial Science and Technology (AIST)
Tsukuba Central 7, Higashi 1-1-1, Tsukuba, Ibaraki, 305-8567, Japan
Phone: +81-29-861-3847
Fax: +81-29-861-3609
E-mail: s.okuma@aist.go.jp

² Geological Survey of Austria
Neulinggasse 38, A-1030 Vienna, Austria

Manuscript received 16 September, 2005.
Revised manuscript received 9 December, 2005.
Part of this paper was presented at the 108th SEGJ Conference (2003).

right-lateral strike slip fault in the Tyrrhenian Sea (Barberi et al., 1994; Ventura, 1994).

Figures 2 and 3 show topographical and surface geological maps of the Vulcano-Lipari complex, respectively.

Vulcano consists of four major volcanic structures whose activity developed between 120 ka and historical times (Ventura, 1994). The southernmost and the oldest structure (120–100 ka; Keller, 1980) is a shoshonitic stratovolcano called Primordial Vulcano (South Vulcano) (Figure 3). At around 100 ka, the upper part of this stratovolcano collapsed and formed a caldera (Piano Caldera) of about 2.5 km in diameter. Piano Caldera was filled by later volcanic activity with tephritic and trachybasaltic lavas, and their pyroclastic deposits. About 24 ka ago, the Lentia volcanic complex was formed by rhyolitic lava, with subordinated latitic and trachytic lavas north of South Vulcano (De Astis et al., 1997). After 15 ka, a collapse of the complex occurred and Fossa Caldera was formed. In the collapsed area, Fossa Cone, a pyroclastic cone with subordinate lava flows, trachytic and rhyolitic in composition, developed in the last 6000 years. In the meantime, the leucite-tephritic activity of Vulcanello occurred at sea north of Fossa Caldera and formed a lava platform covered with pyroclastic deposits (Keller, 1980).

Volcanic activity at Lipari started at around 220 ka (Crisci et al., 1991), with andesitic products on the western coast (Pichler, 1980). The activity of Mt. Sant Angelo volcano in the centre of Lipari lasted until 92 ka (Crisci et al., 1991). After a long quiet period, activity resumed at about 42 ka on the southern part of the island, with rhyolitic lava domes and pyroclastic deposits (Gioncada et al., 2003). After 23.5 ka, the activity yielded rhyolitic fall and surge deposits followed by the extrusion of lava domes (Mt. Guardia and Giardina; Crisci et al., 1991). In the same phase that formed Mt.

Guardia and Giardina, rhyolitic domes (Castello and San Nicola) were formed on the south-eastern side of the island. The most recent volcanic activity on Lipari moved northward (Sheridan et al., 1987). The rhyolitic eruptions occurred from vents aligned along a N-S direction on the east coast, and produced pyroclastic deposits and obsidian lava flows (Gioncada et al., 2003). The latest phase ended with the formation of pyroclastic deposits and a lava flow of the Forgia Vecchia, and a pumice cone (Mt. Pilato) with an obsidian flow (Rocche Rosse).

As described here, the Vulcano and Lipari volcanic complex has been a very active volcanic area and has been studied by many authors. However, the study area, especially close to Fossa Cone on Vulcano, is covered by thick pyroclastic rocks from Fossa and the subsurface structure of the area is not clear. The volcanic rocks on both islands have a wide variety in chemical composition, ranging from rhyolitic to tephritic. However, more mafic rocks are exposed on Vulcano than on Lipari (e.g., Keller, 1980). As mafic rocks are magnetic in general, they can cause apparent magnetic anomalies. Therefore, we conducted aeromagnetic surveys to better understand the subsurface structure of the area.

AEROMAGNETIC SURVEYS

The first helicopter-borne aeromagnetic survey in the Aeolian Islands was conducted over Vulcano and southern part of Lipari

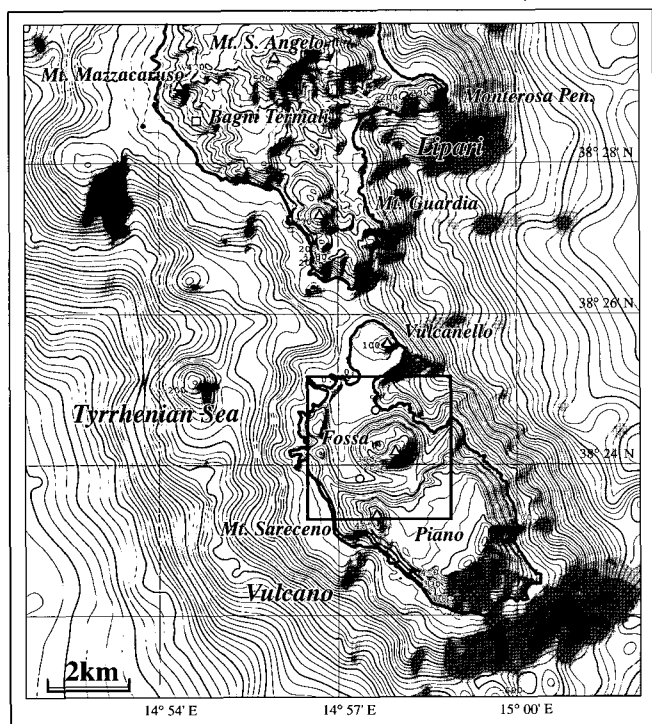


Fig. 2. Topographic map of Vulcano and Southern Lipari, drawn from the 10 m DEM (Gwinner et al., 2000) and a digitised marine chart (Istituto Idrografico Della Marina, 1999). Contour interval is 25 m. The rectangle shows the detailed study area (Figure 8). Open circles indicate the locations of deep geothermal exploration wells.

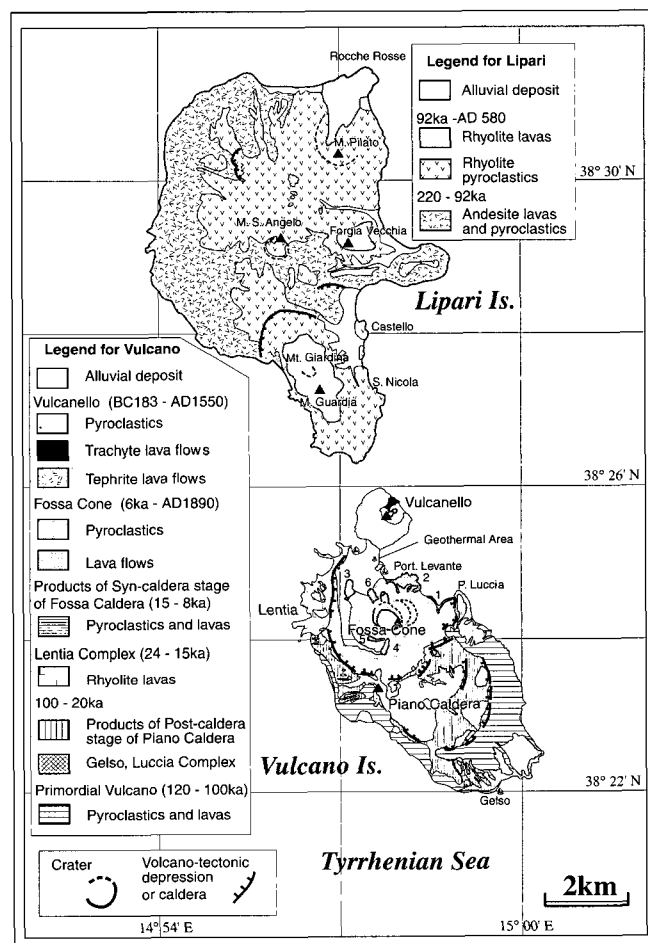


Fig. 3. Simplified geological map of Vulcano and Lipari Islands, Italy, modified from Pichler (1980) and Guest et al. (2003) for Lipari Island, and from Keller (1980) and De Astis et al. (1997) for Vulcano Island. Numbers from 1 to 6 on Vulcano correspond to lava flows — 1: Punta Roia (Tephrite), 2: Punte Nere (Trachyte), 3: Campo Sportivo (Trachyte), 4: Palizzi (Trachyte), 5: Commenda (Rhyolitic Obsidian), 6: Pietre Cotte (Rhyolitic Obsidian).

in 1999 (Supper et al., 2001). The survey was flown with a GLONAS-GPS satellite navigation system at a mean altitude of about 150 m above terrain, along NW-SE flight lines spaced 250 m apart. The magnetic sensor in a bird was suspended 30 m below the survey helicopter. Magnetic data was measured using a Caesium magnetometer at a sampling rate of 10 Hz and with a resolution of 0.01 nT or better. The horizontal location of the flight paths were recovered from GPS data, while terrain clearance was determined using a laser altimeter. The helicopter was also equipped with an infrared video camera to measure the surface signs related to volcanic activity. During the survey period, daily magnetic variation and reference GPS data were observed at a temporary base station next to the heliport on Vulcanello Peninsula.

The second survey was flown in 2002, three years after the first survey, along almost the same flight lines as those of previous survey. In 2002 the locations (latitude, longitude and altitude) of flight line path were determined using real-time Differential GPS. Other survey specifications were basically the same as for the 1999 survey.

MAGNETIC ANOMALIES AND APPARENT MAGNETISATION MAPPING

Observed data were processed and some corrections such as daily magnetic variation, heading error, and IGRF were applied. Magnetic anomalies on a smoothed observed surface were calculated by the reduction method, assuming equivalent anomalies below the observed surface (Makino et al., 1993; Nakatsuka and Okuma, 2005).

The comparison between these magnetic anomaly datasets, observed at two different times separated by three years, identified no meaningful difference related to volcanic activity (Okuma et al., in preparation). On the basis of this result, the two datasets have been merged and total magnetic intensity anomalies on a common surface at an altitude of 150 m above sea level were compiled (Figure 4). The 2002 survey profiles were mainly used for this compilation, with the additional inclusion of four profiles from the 1999 survey to cover a larger area than the individual surveys.

Magnetic terrain corrections (Grauch, 1987) were applied to the merged magnetic anomalies (Figure 4) to reduce the magnetic effects of the terrain, assuming a magnetic structure comprised of an ensemble of prism models extending from the ground surface to a depth of 2000 m below sea level. The depth to bottom was assumed from the observation of a temperature of more than 419°C at the bottom (1975 m BSL) of a geothermal drill hole in the southern foot of Fossa Cone (e.g., Faraone et al., 1986). The optimum magnetisation intensity depends on the area chosen for calculation. It was calculated to be 2.0 A/m for the whole study area, but 3.3 A/m for a limited area of 3.5 km by 3.5 km centred at Fossa Cone. These values seem to be too large for Fossa Cone, which is believed to be composed mainly of pyroclastics (Sheridan et al., 1987). However, the calculated average magnetisation intensity tends to be affected by strongly magnetised bodies even though the size of those bodies is not large. Therefore, an average value for pyroclastics (0.37 A/m; Barberi et al., 1994) was adopted for the terrain correction, and terrain-corrected anomalies were calculated by subtraction of synthetic anomalies from the merged anomalies (Figure 4).

Next, apparent magnetisation intensity mapping (Nakatsuka, 1995) was applied to the terrain-corrected magnetic anomalies. Apparent magnetisation intensities (Figure 5) were calculated assuming the same model as the magnetic terrain correction. Reduction to the pole anomalies on the common surface (Figure 6) were also calculated at the same time as the calculation

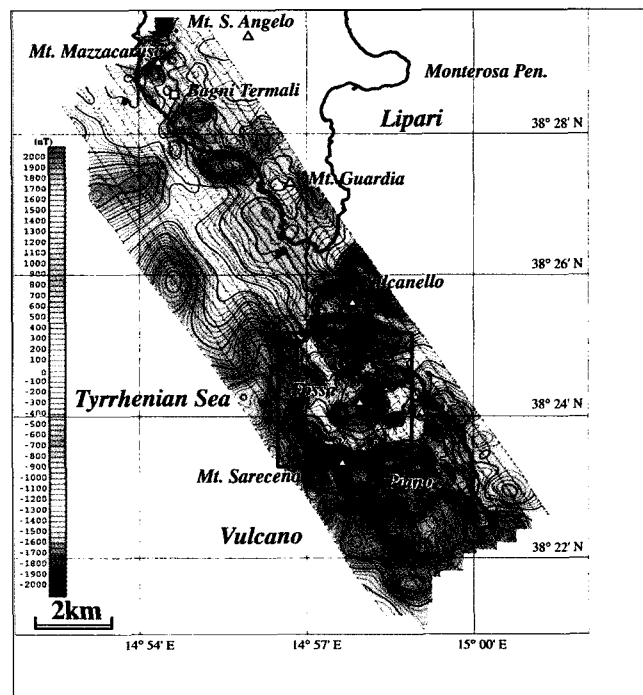


Fig. 4. Aeromagnetic anomaly (total magnetic intensity) map of Vulcano and Southern Lipari, compiled from the merged data from two aeromagnetic surveys which were flown at an altitude of 150 m above terrain with track lines spaced 250 m apart in October, 1999 and November, 2002, respectively. The observed data were reduced onto a smoothed surface 150 m above terrain on land and above sea level at sea. Contour interval is 50 nT. Open red circles indicate the locations of geothermal exploration wells.

of magnetisation intensity (Nakatsuka and Okuma, 2005). Magnetisation intensity mapping is a useful tool to evaluate surface geology and the shallow subsurface structure, as was demonstrated at Izu-Oshima volcano, Japan (Okuma et al., 1994) and at the Kitakami plutons (Okuma and Kanaya, 2005).

The apparent magnetisation intensity map (Figure 5) shows detailed geological signatures. By comparison with a geological map (Figure 3), it can be seen that magnetisation highs lie on trachybasaltic-trachyandesitic lava flows on the flank of Primordial Vulcano. Magnetisation highs (A in Figure 5) are also distributed east and north-east of Sommata inside Piano Caldera, suggesting underlying thick lava flows. Along the rim of Piano Caldera, magnetisation highs also exist, corresponding to exposures of leucite-tephritic lava flows within Piano Caldera (Keller, 1980). These exposures are Schiena Conigliara (B) along the southwestern rim, and Mt. Rosso, Mt. Molineddo (C), and the east flank of Mt. Saraceno (D) along the north-western cliff. A local magnetisation high (E) lies at and around Mt. Lentia, suggesting the existence of a mafic part of the Lentia complex, which is composed mainly of rhyolitic lavas.

Inside Fossa Caldera, scattered magnetisation highs can be identified on and around Fossa Cone. Some of these apparently correspond to lava flows from the Fossa volcano: trachytic lava flows at Punta Nere (F; 5400 ± 1300 YBP) (Frazzetta and La Volpe, 1991; Figure 3) and Campo Sportivo (G; 4600 ± 1950 YBP). No specific signatures were found over a rhyolitic flow (H; Commenda flow; 785 AD) or a trachytic flow (I; Palizzi flow; 1600 ± 1000 YBP) in the southern flank or an obsidian flow (J; Pietre Cotte; 1739 AD) in the northern flank.

An apparent magnetisation high (K) is located east and north-

east of the present crater rim, suggesting the subsurface existence of lava flows covered by younger pyroclastic deposits. A local magnetisation low (L) lies over a cliff between Punta Nere and Punta Roia, corresponding to the April 1988 landslide area (Rasà and Villari, 1991).

A magnetisation high (M) lies on the northern flank between the phreatic craters, Forgia Vecchia I and II (1727 AD) and Porto Levante, suggesting the subsurface existence of magnetic rocks such as lava flows. This area is actually underlain by thick (~400m) latitic lava flows, as confirmed by deep drilling (Vulcano Porto I; Giocanda and Sbrana, 1991). The results of modelling of this magnetisation high are explained in the next section.

The tephritic-trachytic lava platform in the Vulcanello Peninsula is fringed by several magnetisation highs, while a magnetisation low (N) coincides with pyroclastic cones and their surrounding area, indicating magnetic difference in the geology. One of magnetisation highs (O) on the east coast seems to connect to another offshore high (P).

On the west coast of Lipari, magnetisation highs (Q) are distributed in the Mt. Mazzacarus area, corresponding to the exposure of andesitic lavas (cycle I; Pichler, 1980).

The offshore area between Lipari and Vulcano islands is occupied mostly by magnetisation highs but the relationship between magnetisation and submarine topography (Figure 2) is not clear. Offshore and south-west of Lipari, a pair of magnetisation highs (R) occur on the north and south flanks of a ridge. This ridge was identified as a minor volcanic structure during an oceanographic survey (Gabbianelli et al., 1991). Offshore and north-west of Vulcano, magnetisation highs (S) extend from the coast and might indicate basaltic parts of the Lentia volcanic

complex. Offshore of the south-eastern edge of Vulcano lies a magnetisation high (T), which corresponds to a submarine terrace (Gabbianelli et al., 1991), implying its volcanic origin.

The reduction to the pole anomaly map (Figure 6) was used for magnetic modelling. According to the map, there is an obvious regional magnetic difference between the southern Lipari and Vulcano. Magnetic highs are found mainly over Vulcano, though intense volcanic activity has occurred on both islands. This can be interpreted as a petrologic difference between the volcanic rocks composing the two islands. Lipari Island is composed mainly of silicic volcanic rocks such as rhyolites, apart from some andesitic rocks on the west coast, whereas Vulcano Island is composed chiefly of volcanic rocks from trachyte to tephrite, with some minor rhyolite flows.

A similar regional characteristic is also seen in a Bouguer gravity map with an assumed density of $1.8 \times 10^3 \text{ kg/m}^3$ (Figure 7). A regional gravity low lies between Fossa Caldera of Vulcano and Southern Lipari. This feature can be explained by the distribution of rhyolitic volcanic rocks, and the basin-like subsurface structure implied by a velocity model by Ventura et al. (1999). Gravity low areas also occupy the eastern part of Lipari and correspond to the distribution of rhyolitic pyroclastics.

MAGNETIC MODELLING

The apparent magnetisation intensity map (Figure 5) clearly shows the existence and petrographic difference of lava flows at the surface. For instance, the Campo Sportivo trachytic lava flow (Figure 3) corresponds to a magnetisation high while the Pietre Cotte obsidian flow (Figure 3) does not show an obvious magnetic signature. This means that magnetic anomalies can reveal subsurface structure such as concealed magnetic lava flows.

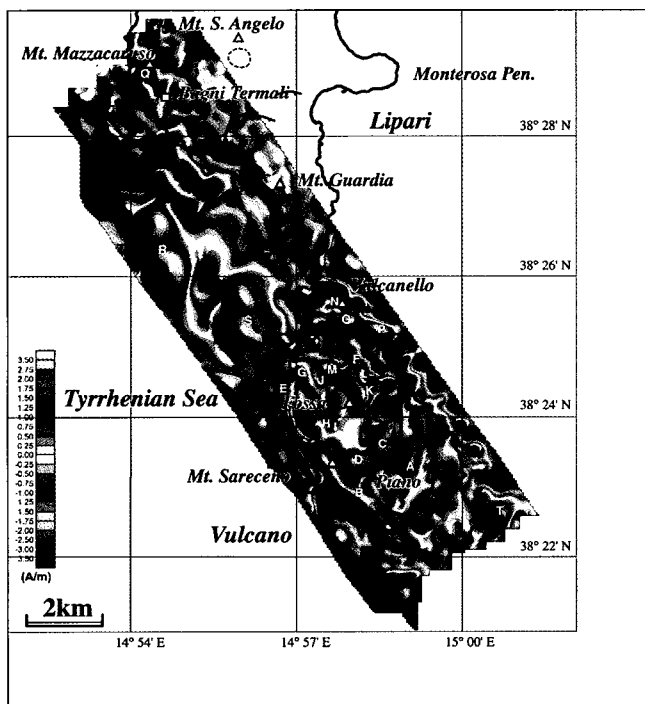


Fig. 5. Shaded relief apparent magnetisation intensity map of Vulcano and Southern Lipari, calculated from terrain-corrected magnetic anomalies with an assumed magnetisation intensity of 0.43 A/m. Letters (A – T) denote characteristics of magnetisation which are referred to in the text. Solid lines, broken lines, and toothed solid lines indicate craters and calderas as in Figure 3.

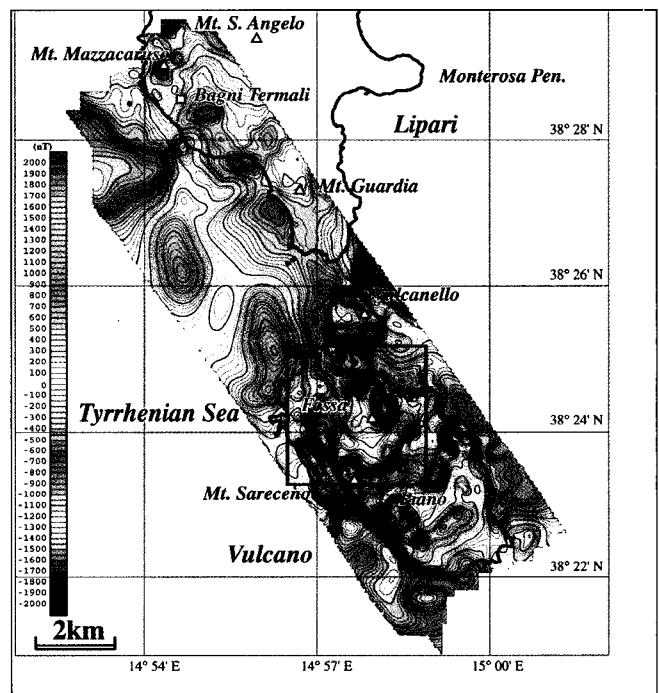


Fig. 6. Reduction to the pole anomaly map of Vulcano and Southern Lipari, calculated from the apparent magnetisation intensity map (Figure 5). The data was reduced onto a smoothed surface 150 m above terrain on land and above sea level at sea. Contour interval is 50 nT.

Magnetic modelling was conducted to constrain the shallow subsurface structure of the Fossa Cone area. We assumed an ensemble of vertical prisms for each layer with the horizontal boundaries deduced from the apparent magnetisation intensity map (Figure 8(a)). This approach is the same as that used by as Okuma and Kanaya (2005) when they conducted modelling of the Kitakami plutons. We allowed variations of top and bottom depths of vertical prisms for each layer. Synthetic magnetic anomalies, which best fit the observed anomalies, were calculated by trial and error, varying also the rock magnetisation data (Barberi et al., 1994, Table 1; Zanella and Lanza, 1994). According to the rock magnetic data reported by Barberi et al. (1994), the mean total magnetisation (the sum of induced and remanent magnetisations) of volcanic rocks from the Aeolian Islands ranges from 0.37 A/m (pyroclastic rocks) to 6.46 A/m (leucite-tephrite). Another study by Zanella and Lanza (1994) reported the measurement of more intense rock magnetic properties on Lipari and Vulcano, although these results were reported without detailed petrographic information.

We used the term “goodness-of-fit” (r) (Blakely, 1995, p224) to judge how well synthetic anomalies (G) fit the observed anomalies (F): the larger the ratio, the better the fit. The goodness-of-fit (r) is defined as

$$r = \frac{\sum_{i=1}^n |F_i|}{\sum_{i=1}^n |F_i - G_i|} \quad (1)$$

We show here the results of magnetic modelling for three areas

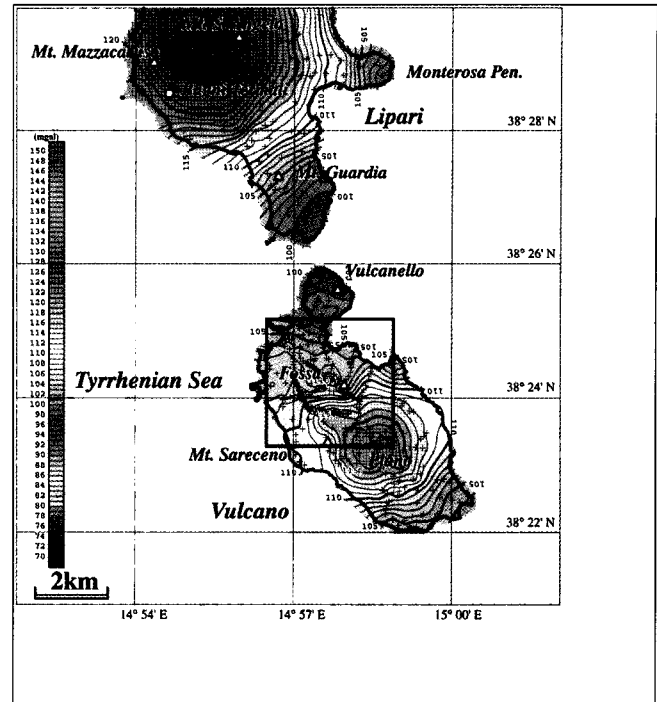


Fig. 7. Bouguer gravity map of Vulcano and Southern Lipari (Sugihara et al., 2002; Komazawa et al., 2003). Assumed density is $1.80 \times 10^3 \text{ kg/m}^3$. Contour interval is 1 mGal. Crosses indicate gravity stations.

on Vulcano: Forgia Vecchia, Fossa Crater, and the NE Fossa Cone. Parameters employed for the magnetic modelling are summarised in Table 2.

Lithology	Number of Samples	Total Magnetisation (A/m)	Bulk Density ($\times 10^3 \text{ kg/m}^3$)
chylolites-dacites	22	2.33	2.31
andesites	24	4.22	2.56
basalts	2	4.88	2.68
trachytes	2	4.81	2.66
latites-latiandesites	14	4.24	2.56
trachybasalts-trachyandesites	9	4.54	2.66
leucite-tephrites	7	6.46	2.13
pyroclastites	12	0.37	N.A.
monzodioritic rock	3	13.58	2.77

Table 1. Petrophysical properties of volcanic rocks from the Aeolian Islands, southern Italy (modified from Barberi et al., 1994).

Parameters		Area A Forgia Vecchia	Area B Fossa Crater	Area C NE Fossa Cone
Layer 1	Top Depth* (m)	50 m ASL	20	10
	Bottom Depth* (m)	Sea Level	45	20
	Total Magnetisation (A/m)	8.0	4.81	4.81
Layer 2	Top Depth* (m)	Sea Level	45	30
	Bottom Depth* (m)	100 m BSL	65	80
	Total Magnetisation (A/m)	8.0	4.81	4.81
Layer 3	Top Depth* (m)	210 m BSL	N.A.	110
	Bottom Depth* (m)	600 m BSL	N.A.	25 m ASL
	Total Magnetisation (A/m)	8.0	N.A.	8.0

Table 2. Parameters used for magnetic modelling. *: Depths are from the ground surface except where noted.

The magnetic model (Figure 9; $r = 1.6$) was constructed by trail and error calculation for Forgia Vecchia on Vulcano (area A in Figure 8), where two phreatic craters reside. An intense magnetisation high is distributed in this area (Figure 8 (a)),

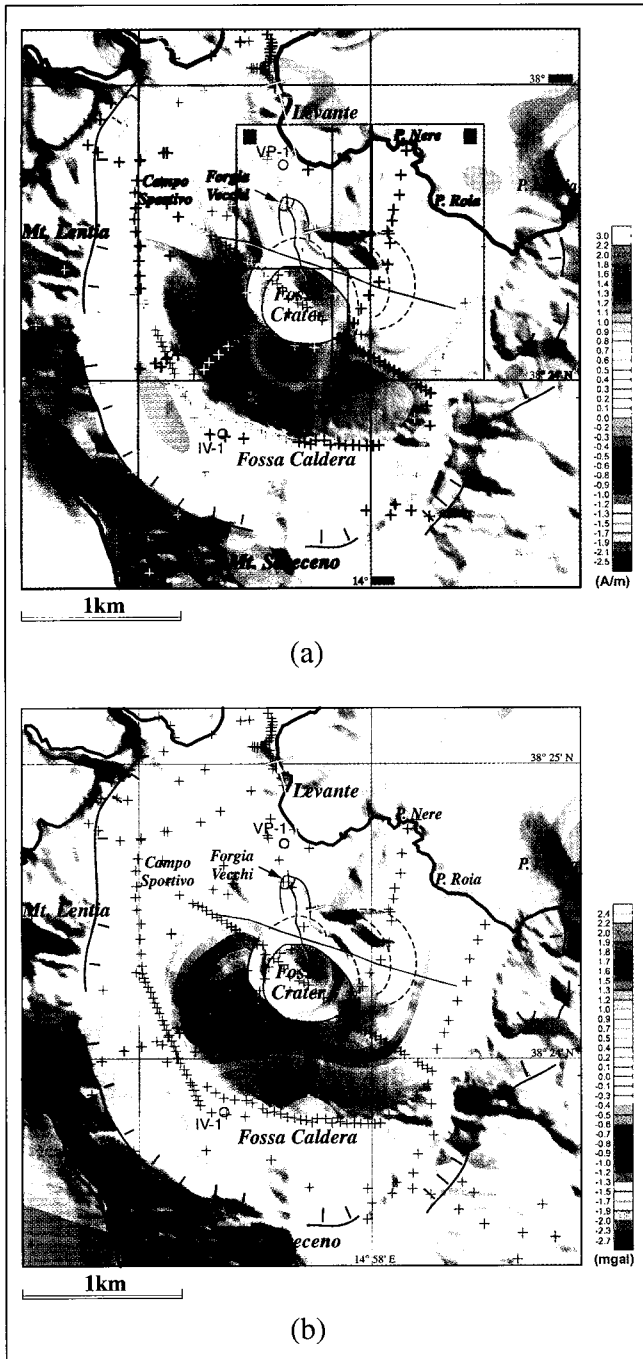


Fig. 8. a) Apparent magnetisation intensity map of the Fossa Caldera area with topographic shading (Gwinner et al., 2000) superimposed. The rectangles indicate magnetic modelling areas. A: Forgia Vecchia area, B: Fossa Crater area, C: NE Fossa Cone area. Craters and volcano-tectonic depressions or calderas are from Keller (1980) and De Astis et al. (1997). The area indicated by a white line shows the distribution of lavas which fill Fossa Caldera, inferred from drilling. Red lines show the survey lines of the geoelectric survey (Supper et al., 2005). Crosses indicate gravity stations. Red open circles labelled VP-1 and IV-1 indicate locations of geothermal exploration wells. See also Figure 3. b) Residual Bouguer gravity anomaly map of the Fossa Caldera area with topographic shading. The first-order regional trend was removed from the Bouguer gravity map (Figure 7). Crosses indicate gravity stations.

although no outcrops associated with magnetic anomalies have been mapped except for an outcrop of Punta Nere trachytic lava flow along the coastline. Information about the lithology obtained from a drill hole (Giocanda and Sbrana, 1991) and residual gravity anomalies (Figure 8(b)) was incorporated into the modelling. The averaged total magnetisation for trachytes of 4.81 A/m (Barberi et al., 1994) was not large enough to explain the magnetic anomalies. Instead, 8.0 A/m, which is an averaged value of tephrites (Zanella and Lanza, 1994), was employed for each layer to fit the anomalies (Table 2). The top and bottom depths of layers 2 and 3 were constrained by drilling. The latitic hyaloclastic layer, at a depth from 100 m to 210 m BSL, was assumed to be non-magnetic.

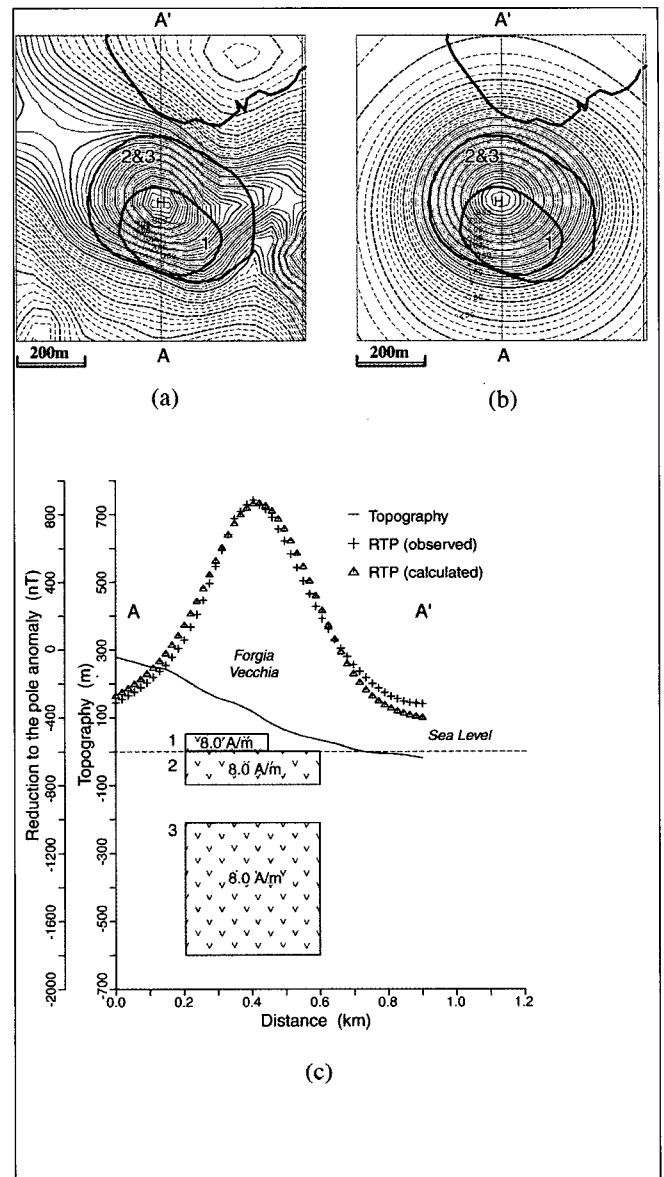


Fig. 9. Magnetic model of the Forgia Vecchia area. a) Reduction to the pole anomalies of the Forgia Vecchia area. Contour interval is 25 nT. The first-order regional trend was removed. Solid lines indicate the horizontal extent of the magnetic models (1–3). The thick solid line shows the coastline. The location of the area corresponds to A in Figure 8(a). See also Figure 8(a). b) Calculated reduction to the pole anomalies of the Forgia Vecchia area. (c) N-S cross section of the magnetic model of the Forgia Vecchia area.

The top and bottom depths of layer 3 are 210 m and 600 m BSL, respectively. The most significant part of this model is layer 1, and the magnetic anomaly cannot be explained without this layer.

Magnetic modelling was conducted for the Fossa Crater area (area B) (Figure 10; $r = 1.7$). The total magnetisation of each layer was assumed to be 4.81 A/m. The top and bottom depths of layer 1 are 20 m and 50 m from the surface, respectively (Table 2), and those of layer 2 are 50 m and 70 m, respectively. This model might imply a concealed trachytic lava flow on the southern edge of the present crater. This model occupies the southern edge of the crater rim of Fossa Cone but is a short distance away from the Commenda rhyolitic lava flow further down the slope.

The magnetic model in Figure 11 ($r = 2.1$) was obtained for the NE Fossa Cone (area C). At first, an averaged total magnetisation of 4.81 A/m for trachytes (Barberi et al., 1994) was employed for

all three layers. In this case, the bottom depth of layer 3 would be as deep as 500 m BSL to fit the observed anomalies. The resultant thickness of this layer might be too thick to explain the gravity low (Figure 8 (b)) lying close to the area. For plutonic rocks, density is roughly proportional to magnetic properties (e.g., Kanaya and Okuma, 2003). However, this relationship does not apply to volcanic rocks such as lavas. Vesicular lavas, or brecciated parts of lava flows like aa lava, are usually magnetic but of relatively low density. This means magnetic but less dense lavas could contribute to high magnetic and low gravity anomalies. However the averaged densities of lavas from the Aeolian Islands are not small (e.g., leucite-tephrites: $2.13 \times 10^3 \text{ kg/m}^3$; Table 1) compared to those of pyroclastic rocks ($\sim 1.8 \times 10^3 \text{ kg/m}^3$). This implies that vesicular or brecciated lavas might be denser than the surrounding pyroclastic rocks in this area. If those lavas are thick, they could cause high gravity anomalies instead of low ones, no matter how deep is the basement of Fossa Caldera in this area. Therefore, to estimate a reasonable thickness, a total magnetisation of 8.0 A/m, which corresponds to an average of tephrite (Zanella and Lanza, 1994), was attributed to layer 3. Magnetisation highs lie on the northern and north-eastern flanks of Fossa Cone and the northern

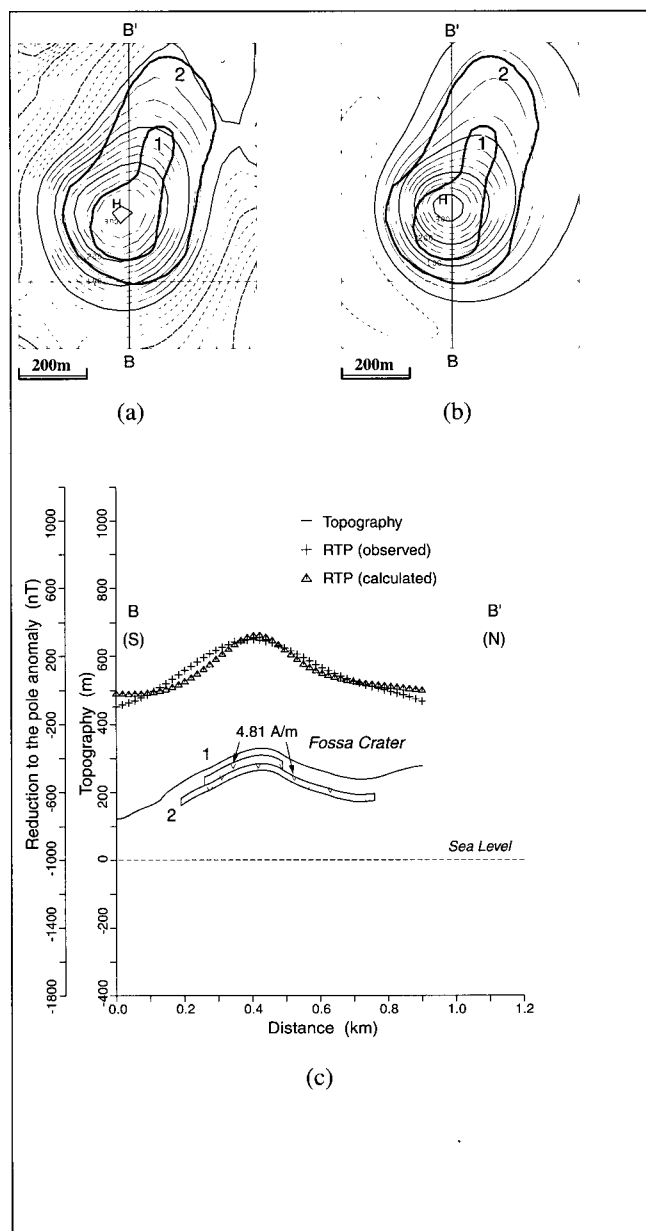


Fig. 10. Magnetic model of the Fossa Crater area. a) Reduction to the pole anomalies of the Fossa Crater area. Contour interval is 25 nT. The first-order regional trend was removed. Solid lines indicate the horizontal extent of the magnetic models (1–2). The location of the area corresponds to B in Figure 8(a). See also Figure 8(a). b) Calculated reduction to the pole anomalies of the Fossa Crater area. c) N-S cross section of the magnetic model of the Fossa Crater area.

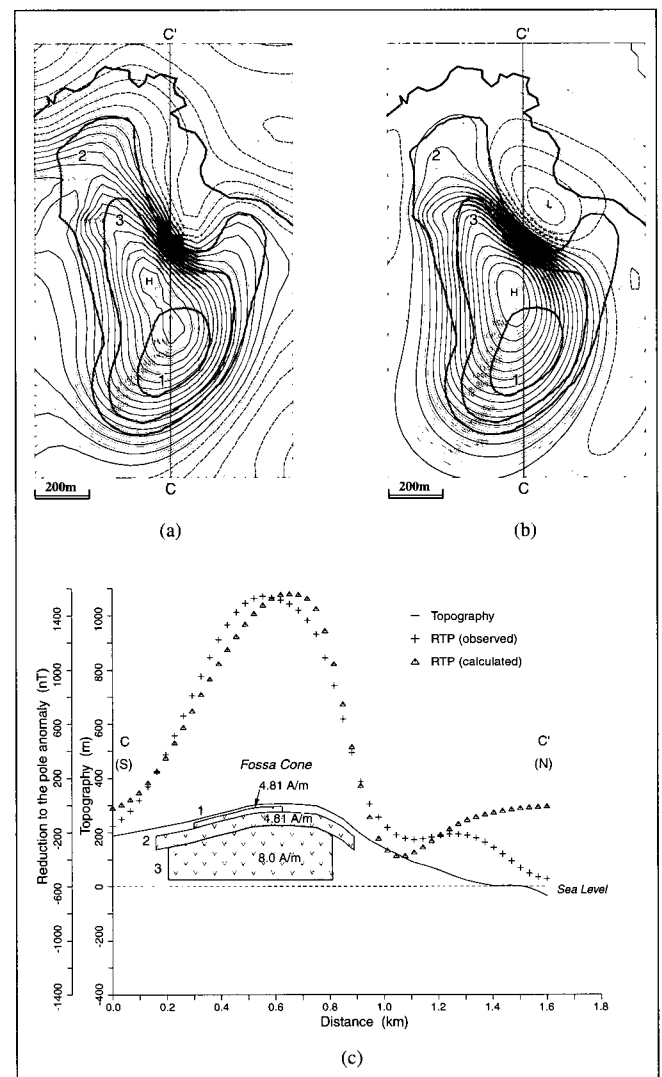


Fig. 11. Magnetic model of the NE Fossa Cone area. a) Reduction to the pole anomalies of the NE Fossa Cone area. Contour interval is 25 nT. Solid lines indicate the horizontal extent of the magnetic models (1–3). The thick solid line shows the coastline. The location of the area corresponds to C in Figure 8(a). b) Calculated reduction to the pole anomalies of the NE Fossa Cone area. c) N-S cross section of the magnetic model of the NE Fossa Cone area.

part seems to reach the distribution area of the Punta Nere trachytic lava flow (Keller, 1980) (Figures 8 and 11). As shown in Figure 8(a), past crater rims were also assumed as well as the present one in this area. The model can account for the subsurface existence of lava flows from past craters, like the Punta Nere lava flow. The north-eastern portion of layer 2 implies another concealed lava flow down to Punta Roia and might be related to the leucite-tephritic lava flow (Punta Roia lava flow; Keller, 1980) which outcrops on the coast from Punta Roia to Punta Luccia.

DISCUSSION

We have conducted magnetic modelling for detailed aeromagnetic anomalies in and around Fossa Cone on Vulcano. The theory of potential fields, applied to magnetic and gravity anomalies, does not guarantee the uniqueness of any solution. Therefore, optimum magnetic models were constructed in areas A, B, and C incorporating rock magnetic data and information from drilling. However, further information is necessary to refine the magnetic models.

Recently, geoelectric surveys have been conducted to determine the structure of hydrothermal systems in Vulcano (Supper et al., 2005). Geoelectric profiles cross the magnetic models in the area A and C and make it possible to compare resistivity and magnetic cross sections. The modelled depths of the resistivity cross-sections are, in practice, 150 to 200 m in these surveys. In area A, a resistivity high of $\sim 100 \Omega \cdot m$ is distributed below Forgia Vecchia, ranging from the bottom right of the cross section (50 m ASL) up to the depth of 25 m below the surface (Figure 12). This resistivity high corresponds to layer 1 of the magnetic model of the area A (Figure 9).

In area C, a resistivity high of 50 to $180 \Omega \cdot m$ also lies below the former rim of the north-east cone. This resistivity high coincides with layer 3 of the magnetic model of the area C (Figure 11).

These magnetic models suggest the presence of volcanic rocks, composed mainly of lavas, overlain by pyroclastics. The Forgia Vecchia satellite cone was produced by two phreatic events that are not directly related to the main eruptive cycles of Fossa Cone

(Frazzetta et al., 1983). No juvenile products were obtained from Forgia Vecchia. However, our results imply magnetic rocks such as lavas (or intrusives) have accumulated both above and below sea level, and these conclusions are supported by the presence of the high-resistivity zone (Supper et al., 2005). It suggests that there might have been very shallow magma intrusions to cause the phreatic explosions which formed Forgia Vecchia, though there is no direct evidence. A local gravity high lies almost in the same area (Figure 8(b)) and suggests some thickness of volcanic layers underneath. This area might be an eruptive centre, obscured by thick pyroclastic products of Fossa.

Giocanda and Sbrana (1991) constructed a N-S geological cross-section of Vulcano, inferred from deep drilling, and showed a distribution of latite rocks within Fossa Caldera which resembled the lava platform of Vulcanello (Figure 8). Our result implies that this distribution is limited to a relatively smaller area than was expected by them. There are two possibilities to explain the difference. One is that intense hydrothermal activity, seen at geothermal areas close to Porto Levante (Figure 3), has caused alteration of the lavas and resulted in the reduction of magnetisation. Another possibility is that thick lavas themselves actually lie within a limited area, although the reason is not clear.

On the other hand, layer 3 of area C implies the presence of thick lavas with high porosity, such as vesicular or brecciated lavas, because relatively low gravity anomalies lie there. The thickness of the lavas was estimated to be about 200 m by magnetic modelling (Figure 11) and at least 175 m by the geoelectric survey (Supper et al., 2005). One of the older rims, right above the magnetic body, is found outside Fossa Cone, (Figure 8) and is thought to be the oldest part of the cone (Frazzetta and La Volpe, 1991). The Punta Nere lava flow (5400 ± 1300 YBP; Figure 3) on the northern slope is thought to have been extruded from the oldest crater. The northern part of layer 2 of area C corresponds to the Punta Nere lava flow. To the north-east of the oldest part of the cone, the Punta Roia lava flow ($14\,000 \pm 6000$ YBP) is exposed on the coastline between Punta Nere and Punta Luccia. On the basis of this information, the magnetic model implies that thick lavas (or intrusives) underlie this area, and may have been another eruptive centre during the period between the extrusion of the Punta Roia and the Punta Nere lava flows.

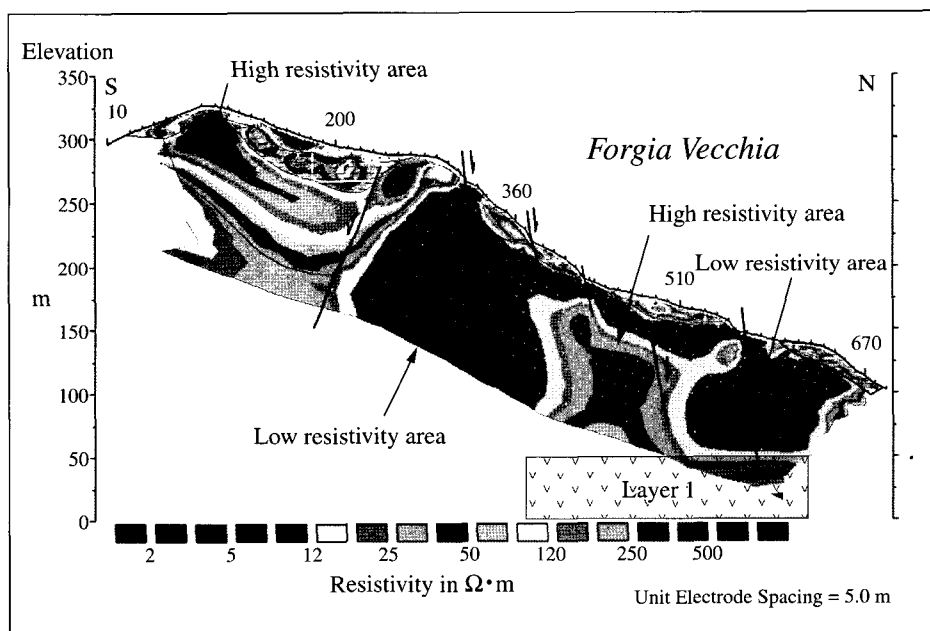


Fig. 12. Geoelectric cross section of Forgia Vecchia (after Supper et al. 2005). Solid lines indicate interpreted faults. Layer 1 of the magnetic model of area A is superimposed. See the location of the cross section in Figure 8.

CONCLUSION

Detailed aeromagnetic anomaly maps in the Vulcano and Lipari volcanic complex area have been compiled. Apparent magnetisation intensity mapping was applied to the terrain-corrected magnetic anomalies and revealed the magnetic signatures of the volcanic rocks on the surface. Magnetisation highs correspond to most outcrops of intermediate to mafic lava flows, while no signatures were observed over rhyolitic lava flows. Magnetic modelling was conducted to constrain the shallow subsurface structure of the Fossa Cone area, incorporating the result of magnetisation intensity mapping, rock magnetic data, geological information, and gravity anomalies. Three concealed magnetic bodies were analysed in this area. The model south of Fossa Crater is thought to be associated with a lava flow from the present crater. The models at Forgia Vecchia on the northern flank of

the cone and north-east of Fossa Cone imply thick lavas overlain by pyroclastic rocks and can be interpreted as eruptive centres in the early stage of the activity of Fossa. As these magnetic models have been found to coincide with high-resistivity zones found by geoelectric surveys, the high-resolution aeromagnetic surveys have successfully revealed the shallow subsurface structure of the area.

ACKNOWLEDGMENTS

This work was supported by the National Institute of Advanced Industrial Science and Technology (AIST), Japan and European Commission, Contract ENV4-CT97-0697 "Electromagnetic and Potential Field Integrated Tomographies Applied to Volcanic Environments - TOMAVE" and by the Austrian Science Found, contract P15515-TEC "Improved Modeling and Interpretation of Complex Geophysical Data Applied to the Eolian Volcanic Province" (COMVOLC). Additional financial support was given by the Austrian Exchange Service (ÖAD).

We express our grateful thanks to Dr. Ichiyo Isobe at the Geological Survey of Japan, AIST, for his helpful comments on the geology of the Aeolian Islands. We further thank Bruno Meurers (University of Vienna) for providing the field transformation algorithm, Serena Diliberto (INGV-Palermo) for providing geochemical data, and Maria Teresa Pareschi for providing the compilation of bathymetric data for the Aeolian Islands. We were grateful for permission from the L'Aquila Geomagnetic Observatory at the Istituto Nazionale di Geofisica e Vulcanologia, Italy to use their digital magnetic data for diurnal magnetic corrections.

REFERENCES

- Barberi, F., Gandino, A., Gioncada, A., La Torre, P., Sbrana, A., and Zenucchini, C., 1994, The deep structure of the Aeolian Arc (Filicudi-Panarea-Vulcano sector) in light of gravity, magnetic and volcanological data: *Journal of Volcanology and Geothermal Research*, **61**, 189–206.
- Blakely, R.J., 1995, *Potential Theory in Gravity and Magnetic Applications*: Cambridge University Press, 441p.
- Crisci, G.M., De Rosa, R., Esperanza, S., Mazzuoli, R., and Sonino, M., 1991, Temporal evolution of a three component system: the island of Lipari (Aeolian Arc, southern Italy): *Bulletin of Volcanology*, **53**, 207–221.
- De Astis, G., La Volpe, L., Peccerillo, A., and Givetta, L., 1997, Volcanological and petrological evolution of Vulcano island (Aeolian arc, southern Tyrrhenian Sea): *Journal of Geophysical Research*, **102**, 8021–8050.
- Faraone, D., Silvano, A., and Verdiani, G., 1986, The monzogabbroic intrusion in the island of Vulcano, Aeolian Archipelago, Italy: *Bulletin of Volcanology*, **48**, 299–307.
- Frazzetta, G., and La Volpe, L., 1991, Volcanic history and maximum expected eruption at "La Fossa di Vulcano" (Aeolian Islands, Italy): *Acta Vulcanologica*, **1**, 107–113.
- Frazzetta, G., La Volpe, L., and Sheridan, M.F., 1983, Evolution of the Fossa Cone, Vulcano: *Journal of Volcanology and Geothermal Research*, **17**, 329–360.
- Furukawa, R., Nakano, S., Okuma, S., and Sugihara, M., 2001, Visiting Cratere; Brief geologic survey at Vulcano Island, Italy: *Chishitsu News*, **559**, 32–40.
- Gabbianelli, G., Romagnoli, C., Rossi, P.L., Calanchi, N., and Lucchini, F., 1991, Submarine morphology and tectonics of Vulcano (Aeolian Islands, Southern Tyrrhenian Sea): *Acta Vulcanologica*, **1**, 135–141.
- Gasparini, C., Iannaccone, G., Scandone, P., and Scarpa, R., 1982, Seismotectonics of the Calabrian Arc: *Tectonophysics*, **84**, 267–286.
- Gioncada, A., Mazzuoli, R., Bisson, M., and Pareschi, M.T., 2003, Petrology of volcanic products younger than 42 ka on the Lipari-Vulcano complex (Aeolian Islands, Italy): an example of volcanism controlled by tectonics: *Journal of Volcanology and Geothermal Research*, **122**, 191–220.
- Giocanda, A., and Sbrana, A., 1991, "La Fossa caldera", Vulcano: inferences from deep drillings: *Acta Vulcanologica*, **1**, 115–125.
- Grauch, V.J.S., 1987, A new variable-magnetization terrain correction method for aeromagnetic data: *Geophysics*, **52**, 94–107.
- Guest, J.E., Cole, P.D., Duncan, A.M., and Chester, D.K., 2003, *Volcanoes of Southern Italy*: Geological Society, London, 284p.
- Gwinner, K., Hauber, E., Jaumann, R., and Neukum, G., 2000, High-resolution, digital photogrammetric mapping: a tool for Earth science: *EOS*, **81**, 44, 513–520.
- Istituto Idrografico Della Marina, 1999, *Isole Di Lipari Vulcano E Salina, Carte Nautiche*, **1:30,000**, 14.
- Kanaya, H., and Okuma, S., 2003, Physical properties of Cretaceous to Paleogene granitic rocks in Japan: Part 1. A case of the northern Tohoku region: *Bulletin of the Geological Survey, Japan*, **54**, 221–233.
- Keller, J., 1980, The island of Vulcano: *Rendiconti della Societa Italiana di Mineralogia e Petrologia*, **36**, 369–414.
- Komazawa, M., Okuma, S., Nakatsuka, T., Sugihara, M., Nakano, S., and Furukawa, R., 2002, Gravity Survey of Vulcano and Lipari Volcano, Italy: *Proceedings of the 106th SEGJ Conference*, 254–257.
- Makino, M., Nakatsuka, T., Morijiri, R., Okubo, Y., Honkura, Y., and Okuma, S., 1993, Derivation of three-dimensional distribution of geomagnetic anomalies from magnetic values at various elevations: *Proceedings of the 88th SEGJ Conference*, 502–507.
- Nakatsuka, T., 1995, Minimum norm inversion of magnetic anomalies with application to aeromagnetic data in the Tanna area, Central Japan: *Journal of Geomagnetism and Geoelectricity*, **47**, 295–311.
- Nakatsuka, T., and Okuma, S., 2006, Reduction of magnetic anomaly observations from helicopter surveys at varying elevations: *Exploration Geophysics*, **37**, (this issue).
- Okuma, S., and Kanaya, H., 2005, Utility of petrophysical and geophysical data to constrain the subsurface structure of the Kitakami plutons, northeast Japan: *Earth, Planets and Space*, **57**, 727–741.
- Okuma, S., Makino, M., and Nakatsuka, T., 1994, Magnetization intensity mapping in and around the Izu-Oshima volcano, Japan: *Journal of Geomagnetism and Geoelectricity*, **46**, 541–556.
- Okuma, S., Nakatsuka, T., Sugihara, M., Komazawa, M., Nakano, S., Furukawa, R., Elenjiparampil, E.J., Supper, R., and Chiappini, M., 2003, *Geophysical Signature on the Subsurface Structure of the Aeolian Islands, Italy*: IUGG 2003 Abstracts Week B, B.256.
- Pichler, H., 1980, The island of Lipari: *Rendiconti della Societa Italiana di Mineralogia e Petrologia*, **36**, 415–440.
- Rasà, R., and Villari, L., 1991, Geomorphological and morpho-structural investigations on the Fossa Cone (Vulcano, Aeolian Islands): a first outline: *Acta Vulcanologica*, **1**, 127–133.
- Sheridan, M.F., Frazzetta, G., and La Volpe, L., 1987, Eruptive histories of Lipari and Vulcano, Italy, during the past 22,000 years: in Fink, J.H. (ed.), *The emplacement of Silicic Domes and Lava Flows: Geological Society of America, Special Paper*, **212**, 29–34.
- Sugihara, M., Okuma, S., Nakano, S., Furukawa, R., Komazawa, M., and Supper, R., 2002, Relationship between geothermal activity and gravity anomalies on Vulcano Island, Italy: *Proceedings of the 24th NZ Geothermal Workshop*, 175–179.
- Supper, R., Deritis, R., and Chiappini, M., 2004, Aeromagnetic anomaly images of Vulcano and Southern Lipari Islands (Aeolian Archipelago, Italy): *Annals of Geophysics*, **47**, 1803–1810.
- Supper, R., Motschka, K., Seiberl, W., and Fedi, M., 2001, Geophysical investigations in Southern Italian active volcanic regions: *Bulletin of the Geological Survey, Japan*, **52**, 89–99.
- Supper, R., Stotter, C., and Gwinner, K., 2005, Geoelectric surveys to supplement to determine the structure of hydrothermal systems – Case Study Vulcano: *Proceedings of 11th meeting of Environmental and Engineering Geophysics*, Palermo, Italy, EAGE Near Surface Div., A010.
- Ventura, G., 1994, Tectonics, structural evolution and caldera formation on Vulcano Island (Aeolian Archipelago, southern Tyrrhenian Sea): *Journal of Volcanology and Geothermal Research*, **60**, 207–224.
- Ventura, G., Vilardo, G., Milano, G., and Pino, N.A., 1999, Relationships among crustal structure, volcanism and strike-slip tectonics in the Lipari-Vulcano Volcanic Complex (Aeolian Islands, Southern Tyrrhenian Sea, Italy): *Physics of the Earth and Planetary Interiors*, **116**, 31–52.
- Zanella, E., and Lanza, R., 1994, Remanent and induced magnetization in the volcanites of Lipari and Vulcano (Aeolian Islands): *Annali di Geofisica*, **37**, 5, 1149–1156.

**ヘリボーン空中磁気探査により推定された
イタリア・ブルカノーリパリ複合火山体の浅部地下構造**
大熊茂雄¹・中塚 正¹・駒澤正夫¹・杉原光彦¹・中野 俊¹・古川竜太¹・R. スッパ²

要 旨： イタリア・エオリア諸島において、ブルカノーリパリ複合火山体の浅部地下構造を明らかにし、また当該地域の火山活動をモニタリングする目的で、3年間の間隔をおいて2回のヘリボーン空中磁気探査が行われた。2回の調査データを比較したところ火山活動の変化に対応すると考えられる顕著な磁気異常の変化は認められなかったため、両調査データを取り込んでより広範囲をカバーする空中磁気異常図が作成された。次にこの磁気異常データに地形補正を施した後、磁化強度マッピングを行ったところ、ブルカノ島のフォッサ火砕丘およびその周辺で、その磁氣的不均質を示す複数の局所的高磁化強度域が分布することが明らかとなった。これらのうち3カ所の高磁化強度域について磁気構造を解析したところ、フォッサ火山体からの大量の火砕物に覆われた高磁性の火山岩類が伏在することが推定された。フォッサ火口では、現在の火口中心から南外縁部外側斜面にかけてトラカイト溶岩流の伏在が示唆された。また、フォッサ火砕丘の北側斜面の爆裂火口であるフォルジア・ベッキアは、単なる爆裂火口ではなく、フォッサカルデラを埋積する厚いレタイト溶岩を噴出した噴火中心であったことが推定された。ただし、磁気構造からは、ボーリングデータにより推定された同溶岩の分布範囲が予想より局所的である可能性が示された。その原因の一つとしては、当該地域のレバンテ港付近の地熱地帯にみられるような活発な熱水活動により溶岩が変質し磁化を弱めていることが考えられる。一方、フォッサ火砕丘の北東部でも、厚い溶岩/貫入岩の存在が解析され、当該地域はフォッサ火山体の活動初期(約5,500年前)に形成されたと考えられることから、当時の噴火中心の一つであったと推定される。かつての噴火中心と解釈されたこれら2地域では、最近地上電気探査が実施され、いずれも高比抵抗層が分布することが明らかとなり、ヘリボーン空中磁気探査の結果を支持している。

キーワード： 火山帯地下構造、磁気異常、空中磁気探査、エオリア諸島、ブルカノーリパリ複合火山体

고해상도 항공자력탐사를 이용한 Italia Vulcano-Lipari 화산 복합체의 천부 지하 구조
Shigeo Okuma¹, Tadashi Nakatsuka¹, Masao Komazawa¹, Mitsuhiro Sugihara¹,
Shun Nakano¹, Ryuta Furukawa¹, and Robert Supper²

요 약： 남부 Italia Aeolian 군도의 Vulcano-Lipari 화산 복합체의 천부 지하구조를 잘 이해하고 또한 이 지역의 화산활동을 모니터링하기 위해서 고해상도 항공자력탐사가 3년간의 간격을 두고 두 번 수행되었다. 두 개의 서로 다른 자력탐사 자료가 화산활동의 변화를 지시하는 어떠한 의미있는 차이를 보이지 않기 때문에, 자료들은 서로 합쳐져서 단일 자료보다 넓은 영역에 대한 항공자력도로 만들어졌다. 지형보정된 자력이상으로부터 걸보기 자화강도 분포도가 만들어졌으며 이로부터 Fossa 원추구의 이질성을 제시하는 국부적인 고 자화 이상을 볼 수 있었다. 이 중 세 개의 고 자화 이상에 대해 자력 모델링이 수행되었다.

각 모델은 Fossa 화구의 화산쇄설류로 덮혀있는 화산생성물의 존재를 밝히는 데에 적용되었다. Fossa 화구 지역에 대한 모델로부터 현재 화구의 남쪽 가장자리에는 조면암질 용암류가 묻혀있다는 것이 제시되었다. Forgia Vecchia 에서 적용한 자력모델은 수증기 폭발성 원추구가, Fossa 칼데라를 메운 레타이트질 용암류(현무암질조면암과 안산암질조면암을 통칭)에 덮혀버린 한 분출중심으로부터 형성되었다는 것을 제시해 준다. 하지만 용암류의 분포는 기존의 시추 결과들로부터 알려진 것보다도 적은 지역에 국한되는 것처럼 나타난다. 이는 Porto Levante 에 인접한 지열지역에서 알 수 있듯이, 강렬한 열수활동으로 인한 용암류의 부분적인 변질에 기인한 것으로 설명될 수 있다. Fossa 원추구 북동부에서의 모델은 두꺼운 용암류가 Fossa 화산활동의 초기단계에 또 다른 분출중심에서 집적되어 있다는 것을 암시한다. 최근의 전기탐사는 마지막 두 자력모델 지역에서 고비저항대를 보여준다.

주요어： 고해상도 항공자력탐사, Vulcano, Lipari, Aeolian 군도

1 産業技術総合研究所 地質情報研究部門
〒305-8567 茨城県つくば市東 1-1-1 中央第 7
2 オーストリア地質調査所

1 산업기술종합연구소 지질정보연구부문
2 오스트리아 지질조사소